Effects of Hydration on the Properties of Protonated-Water−Nitric Acid Clusters

Raffaella D'Auria* and Richard P. Turco

Department of Atmospheric, Oceanic and Environmental Sciences, University of California, Los Angeles, Los Angeles, California 90095-1565

K. N. Houk

Department of Chemistry and Biochemistry, University of California, Los Angeles, Los Angeles, California 90095-1569

Received: November 20, 2003; In Final Form: February 17, 2004

The uptake of nitric acid by protonated water (hydronium cation, H_3O^+) clusters and the characteristic structures of the resulting mixed aggregates, $H^+\cdot(H_2O)_n\cdot(HNO_3)_m$, have been studied theoretically. As baseline simulations, B3LYP/6-311++G(d,p) geometry optimizations and energy calculations for $n = 1-9$ and $m = 0-1$ have been employed. To establish the mechanism of nitric acid uptake by hydronium ion−water clusters, the energetics of the various reaction pathways involving $H_3O^+\cdot(H_2O)_n$ and HNO_3 are evaluated. In the presence of hydronium ion−water clusters, protonated nitric acid forms by a charge exchange reaction involving H_3O^+ and HNO_3. Successive hydration of $H^+\cdot HNO_3$ is an energetically favorable phenomena resulting in the formation of the mixed clusters containing one nitric acid molecule. However, when the number of water ligands on the clusters is less than about five, water binds more strongly to protonated water aggregates than to the mixed clusters. Accordingly, water will preferentially react with hydrated hydronium ions. Attachment reactions of nitric acid to the hydronium ion−water clusters are also found to be exothermic across the spectrum of sizes considered. However, switching reactions, involving H_2O and $H^+\cdot(H_2O)_n\cdot(HNO_3)$ for $n = 2-7$, are found to reestablish the hydronium ion−water cluster series. Above five water molecules, the binding energy of water to the mixed clusters containing one nitric acid molecule becomes comparable to that of the equivalent water aggregates; hence, the concentration of the former is expected to grow. Similar behavior has been experimentally observed by Castleman and co-workers [Zhang, X.; Mereand, E. L.; Castleman, A. W., Jr. *J. Phys. Chem.* **1994**, *98*, 3554. Gilligan, J. J.; Castleman, A. W., Jr. *J. Phys. Chem. A* **2001**, *105*, 5601].[1,2] The structural arrangement of the optimized mixed clusters has also been investigated. The results show that isomeric configurations exist and that, depending on the degree of hydration of the ionic clusters, the most stable structures are the hydronium ion (H_3O^+), $H_5O_2^+$ or the nitronium ion (NO_2^+). For low levels of hydration (i.e., $n = 0, 1$), the nitronium ion−water structures appear to be the most stable. These results agree with experimental investigations [Cao, Y.; Choi, J.-H.; Haas, B.-M.; Johnson, M. S.; Okumura, M. *J. Chem. Phys.* **1993**, *99*, 9307. Cao, Y.; Choi, J.-H.; Haas, B.-M.; Okumura, M. *J. Phys. Chem.* **1994**, *98*, 12176. Choi, J.-H.; Kuwata, K. T.; Cao, Y.-B.; Haas, B.-M.; Okumura, M. *J. Phys. Chem. A* **1997**, *101*, 6753].[3−5] The geometry optimized structures also show that, depending on the cluster arrangement, the nitric acid molecule can dissociate into NO_3^- and H_3O^+ when the number of water ligands in the cluster is greater than about seven.

Introduction

Given the importance of atmospheric aerosol containing nitrate−water mixtures, understanding the mechanism of heterogeneous condensation of water and nitric acid is a critical step in the overall comprehension of the atmospheric aerosol formation process. We report a theoretical study aimed to unravel the characteristics of nitric acid condensation onto protonated water clusters. These aggregates are common in the atmosphere due to the continuous generation of ion pairs under the action of the galactic cosmic rays (and other local minor sources) and the subsequent series of fast reactions which transform the newly generated ions into protonated water (i.e., the hydronium ion). This ion, depending on the environmental conditions, can further cluster with water and/or undergo switching reactions with other atmospheric trace constituents.[6] The atmospheric population of hydronium ion−water clusters typically includes aggregates with dimensions lying in the prenucleating segment of the overall atmospheric particulate size distribution. This population is stable, since the total Gibbs free energy change associated with the formation of the clusters, $\Delta G_{0,n}$, exhibits a minimum at such cluster sizes. In general, for nucleation precesses, the total Gibbs free energy change associated with the formations of clusters has a maximum for a certain number of ligand molecules known as the critical number. The maximum represents the barrier toward spontaneous particulate growth (i.e., nucleation) unless environmental conditions are largely supersaturated with respect to the condensing vapor, in which case nucleation occurs freely. The appearance of a minimum in the total Gibbs free energy curve,

* To whom correspondence should be addressed. E-mail: dauria@atmos.ucla.edu. Phone: +1-310-825-9230. Fax: +1-310-206-5219.

10.1021/jp037543q CCC: $27.50
Published on Web 04/06/2004

for the pre-nucleating aggregate size range, is a distinct signature of the presence of a core ion and is absent for neutral aggregates. In the atmosphere different families of mixed ionic clusters have been measured (e.g., refs 7−10), but the impact of these clusters on atmospheric particulates has not yet been fully addressed. Charged molecular aggregates are likely to have a role in atmospheric nucleation phenomena.

Specifically, hydronium ion−water−nitric acid clusters in the polar winter stratosphere may act as polar stratospheric clouds (PSCs) type Ia (thought to be composed of crystalline nitric acid hydrates) condensation nuclei and thus indirectly influence the polar stratospheric ozone loss process. The clusters studied here can also be taken as proxies for the behavior of matter on atmospheric aerosol surfaces, where dissolution of acids and other airborne components takes place with the formation of localized ion pairs. Consequently, knowledge of the physical behavior of ionic clusters can lead to a more general description of the chemistry of acid dissolution on aerosol surfaces. In this paper, the properties of the water−nitric acid cation clusters are evaluated as a step toward proper modeling of the role of such aggregates in the atmospheric aerosol budget.

The first experimental investigation of the gas-phase ion chemistry of nitric acid was carried out by Fehesenfeld et al.[11] Using flowing afterglow ion mass spectrometry techniques, the authors studied the properties of protonated nitric acid, $H^+\cdot HNO_3$, and hydrated nitronium ion, $NO_2^+\cdot H_2O$, which were produced by independent processes. Because the two ion products were found to have the same behavior, Fehesenfeld et al. concluded that these species are chemically equivalent. This conclusion was later supported by both theoretical studies (e.g., ref 12) and laboratory measurements.[3−5,13−15] In their experiments, Fehesenfeld and co-workers detected no $H^+\cdot HNO_3\cdot H_2O$, which they believed was formed upon attachment of water to protonated nitric acid. They concluded that, upon hydration, protonated nitric acid efficiently switches its charge with water (i.e., transfers a proton), releasing nitric acid and forming $H_3O^+\cdot H_2O$. This transformation occurs so efficiently that the concentration of hydrated protonated nitric acid clusters is too low to be detected. In the same paper, Fehesenfeld et al. also reported the first inferred value for the proton affinity of nitric acid, 176 ± 7 kcal/mol, which is consistent with other estimates.[14−16]

Subsequently, Castleman and co-workers[1,2] examined the reaction mechanisms of nitric acid with protonated water clusters up to thirty water ligands at thermal conditions by means of ion mass spectrometry techniques. To avoid mass degeneracy, which would lead to ambiguous mass spectra, deuterated water and deuterated nitric acid were used. In these studies, a stable distribution of hydronium ion−water clusters is exposed to nitric acid vapors. At equilibrium, the products contain both hydronium ion−water clusters and mixed charged water−nitric acid clusters. The distribution of the mixed clusters, however, is not continuous. Mass peaks are observed for the protonated nitric acid, $D^+\cdot DNO_3$, and for $D^+\cdot(D_2O)_n\cdot DNO_3$ when $n \geq 5$, for $D^+\cdot(D_2O)_n\cdot(DNO_3)_2$ when $n \geq 8$, and for $D^+\cdot(D_2O)_n\cdot(DNO_3)_3$ when $n \geq 13$. This implies that at least five water ligands must be present about the proton before the first nitric acid molecule is taken up by the hydronium ion−water cluster. Eight waters are necessary before a second acid molecule condenses, and thirteen are required before the third HNO_3 can be incorporated. When the experiment was performed "with a very small amount of water vapor" and at room temperature, only the presence of the hydronium ion was recorded. After the introduction of DNO_3, protonated nitric acid was detected but, in agreement with the previously discussed results of Fehesenfeld and co-workers, $D^+\cdot(DNO_3)\cdot(D_2O)$ was not detected. When higher concentrations of water were present, $D_3O^+\cdot(D_2O)_n$ clusters, with n ranging from 1 to 3, were observed. In this case, the introduction of nitric acid did not produce any detectable reactions. However, when the temperature was lowered below 180 K, and larger hydronium ion−water clusters appeared, the introduced nitric acid vapor was incorporated into the hydronium ion−water clusters containing at least four water ligands (or, equivalently, into $D^+\cdot(D_2O)_n$ aggregates with $n \geq 5$). To understand the reaction mechanisms, Castleman and co-workers repeated the experiments varying the total pressure in the flow tube from 0.3 to 0.8 Torr. Because the reactions did not show signs of pressure dependence, Castleman and co-workers concluded that the uptake of nitric acid involves a switching between the condensing nitric acid molecule and a water ligand, rather than a direct association of the former on the protonated water cluster (association reactions generally display faster rates at higher pressures).

Okumura and co-workers[3−5] have reported the results of predissociation vibrational spectroscopy experiments regarding protonated nitric acid clusters. The authors observed that, when irradiated with photons having energies in the IR spectrum, $H^+\cdot HNO_3\cdot(H_2O)_n$ clusters dissociate along two primary routes depending on the value of n. For $n = 1$ or 2, water dissociation is the dominant mechanism, indicating that the clusters are mainly nitronium ion−water adducts. For $n > 2$, nitric acid is the major dissociation product, indicating that these clusters conform to a hydronium ion−water aggregate weakly bound to a nitric acid molecule.

We report a computational study aimed to understand and characterize the structure and behavior of mixed water and nitric acid ionic clusters. The energetics of such clusters are described first, to asses the reaction mechanisms that are likely to control nitric acid uptake by hydronium ion−water cluster. This includes estimating the computational error to attribute to the computed energetics. Then the structural arrangements of the two different families of clusters studied (protonated water and mixed aggregate) are described in detail, and the findings are compared with laboratory data.[3−5,17−19] Evidence is presented for the dissociation of nitric acid within the mixed clusters with the consequent formation of a second hydronium ion. We conclude that formation of charge pairs in such mixed clusters occurs when the number of water ligands in the aggregate is equal to or greater than seven, and the water molecules form a cage-like structure about the acid molecule.

Computational Details

Geometry optimizations and frequency calculations on the hydronium ion−water and the mixed clusters were performed with B3LYP hybrid density functional theory and the 6-311++G(d,p) basis set within the Gaussian 98 suite of programs.[20] The enthalpy changes associated with the clustering reactions were computed as the differences between the enthalpies of the products and the reactants

$$\Delta H = \sum_{\text{products}} (\epsilon_0 + E_{\text{tot}} + k_B T) - \sum_{\text{reactants}} (\epsilon_0 + E_{\text{tot}} + k_B T) \quad (1)$$

where ϵ_0 is the total electronic energy, E_{tot} is the internal thermal energy (sum of the translational, rotational and vibrational contributions), T is the temperature, and $H_{\text{corr}} = E_{\text{tot}} + k_B T$ is the thermal correction to the enthalpy. Since we are interested in comparing our calculations to the laboratory results of Castleman and co-workers,[1,2] the frequency analysis was

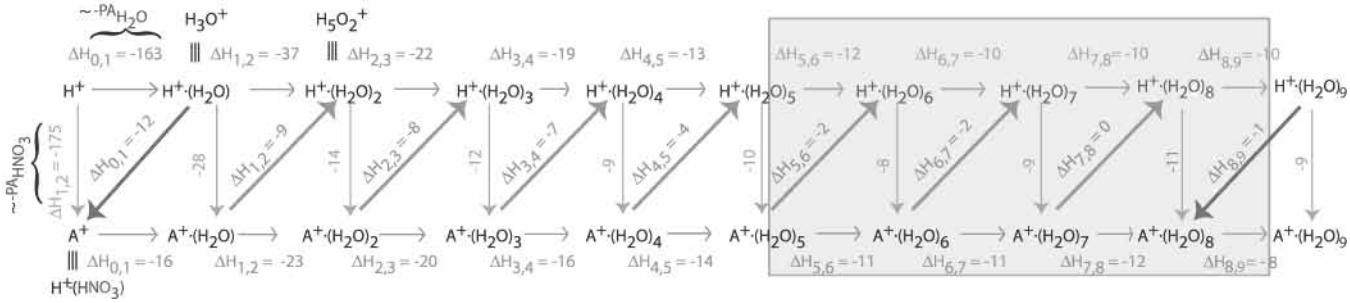

Figure 1. Schematic summary of the possible reaction pathways and the enthalpy changes (in kcal/mol) associated with them. The arrows are pointed in the direction for which the reactions are exothermic. For brevity, protonated nitric acid, $H^+ \cdot HNO_3$, is represented by the cation A^+. The shaded box toward the right shows enthalpy values for switching reactions that are within the computational errors. The values reported here are obtained for $T = 156$ K and $p = 0.36$ Torr. Hence, the negative of the enthalpy values for the hydration/uptake of nitric acid of the proton are related to the actual proton affinities of water and nitric acid (which are reported below in Table 1 and 2).

performed at the temperature and pressure of the experiments (i.e., $T = 156$ K and $p = 0.36$ Torr).

Our calculations have not been corrected for the basis set superposition error (BSSE) because it is likely that such a correction would result in a value smaller[21] than the estimated error attributed to the computational technique (see later).

Results and Discussion

Energetics. To evaluate the actual reaction pathways that involve hydronium ion−water clusters interacting with nitric acid vapor, the free energy changes associated with each possible clustering reaction have been evaluated. Since the calculations are carried out at low temperature ($T = 156$ K), the entropy makes a relatively small contribution to the overall reaction energetics; hence, we focus on the enthalpic contribution to cluster stability. The basis for this approach is further justified in a separate manuscript in preparation. There are two aggregation mechanisms that have to be taken into account: (1) an association reaction, for which a ligand directly bonds to the preexisting cluster, and (2) a switching reaction, in which the condensing species (e.g., nitric acid) replaces one of the ligands (here water) of the cluster. The latter process also includes charge exchange reactions as in the formation of protonated nitric acid from hydronium ion.

Results from these calculations are summarized in Figure 1. The upper horizontal portion of the graph shows the results for the clustering of water onto proton hydrates ($H^+ \cdot (H_2O)_{n-1} + H_2O \rightleftharpoons H^+ \cdot (H_2O)_n$). The negative value of the enthalpy change associated with the hydration of a proton is, at standard conditions, the proton affinity of water (PA_{H_2O}). The bottom horizontal segment of the figure represents the hydration reactions of protonated nitric acid (designated as A^+ in the figure). Vertical arrows represent the association reactions of nitric acid to protonated water aggregates to yield protonated nitric acid clustered with water. The negative value of the enthalpy change associated with the uptake of nitric acid of the proton is the proton affinity of nitric acid (PA_{HNO_3}). Finally, the sideways arrows indicate switching reactions (i.e., $H_3O^+ + HNO_3 \rightleftharpoons H_2NO_3^+ + H_2O$, etc.). Each enthalpy value reported in Figure 1 is the Boltzmann average over the isomers identified in the geometry optimizations (discussed below).

The results shown in Figure 1 confirm that the successive hydration steps of both protonated water clusters and mixed aggregates are exothermic processes. In particular, the enthalpy changes associated with the hydration reactions are greater for the protonated water clusters up to four water ligands (i.e., $H^+ \cdot (H_2O)_4$), whereas beyond five water ligands, the enthalpy difference values for both hydration processes become similar. Hence, at a low level of hydration, water bonds more strongly to protonated water clusters than to mixed clusters, and the populations of clusters containing less than five water ligands are richer in the hydronium ion−water aggregates.

The second inference from Figure 1 is that hydronium ion readily exchanges its proton with nitric acid to form protonated nitric acid, since the proton affinity of nitric acid is greater than that of water.[22] However, when protonated nitric acid is hydrated, the switching reactions, for the clusters containing one to seven ligands, occur in the opposite direction. Therefore, for that size range, the proton affinities of mixed clusters are smaller than these of protonated water clusters with the same number of ligands. The proton affinity is clearly a function of the degree of hydration of the aggregate.

Castleman and co-workers[1,2] predict that, for more than five water ligands on a proton, the switching reactions favor the formation of mixed clusters. In Figure 1, for five, six, and seven water ligands on a cluster, the switching reactions favor the formation of hydronium ion−water clusters. However, the exothermicities are within the computational error (see the discussion below), and the exothermic direction of these reactions is ambiguous in these cases. Assuming the computational error to be about 3 kcal/mol (see next section), these reactions could be nearly thermoneutral or slightly exothermic favoring the mixed cluster formation. The switching reaction between the proton hydrate cluster with eight water ligands and the mixed cluster with seven is predicted to be thermoneutral. The switching reaction between the protonated water cluster composed of nine ligands and the mixed cluster containing eight water molecules is exothermic in the direction favoring the mixed clusters (again, within the computational error).

In conclusion, we have investigated the possible pathways to nitric acid deposition onto water proton clusters. Switching reactions that favor nitric acid uptake by hydronium ion clusters happen when a certain number of water ligands are present in the aggregate (although this number could not be determined unambiguously in our study). This suggest that proton hydrates in the atmosphere grow by nitric acid deposition following certain nitric acid-to-water ratios. A kinetic study of such clustering mechanism is under way to address its possible implications on the formation of polar stratospheric clouds type Ia composed of crystalline nitric acid hydrates.

Estimate of the Computational Error. There is a significant body of data regarding the energetics of the formation of hydronium ion−water aggregates (see, for example, Kebarle and co-workers[23−25] and others).[26−45] A comparison of the computed thermochemical properties with the experimental data has been used to estimate the computational error. For this

TABLE 1: Enthalpy Changes and Deviations in kcal/mol Approximated to the Most Significant Digit (with the Exception of Cases in which the Most Significant Figure Is the Number 1 or 2 in which Cases Two Significant Figures Are Retained)[a]

no. of ligands	data averages and standard deviations						computed averages and deviations from data				
$(n-1,n)$	$\overline{\Delta H^0_{n-1,n}}$	$\pm\sigma_n$	N	$\overline{\Delta H^0_{n-1,n}}'$	$\pm\sigma_n'$	N'	$\langle\Delta H^0_{n-1,n}\rangle$	da_n	dr_n	da_n'	dr_n'
$(-1,0)^b$	−165[c]		1	−165[c]		1	−166	1	6	1	6
(0,1)	−30	10	18	−33.4	2.4	11	−37.0	10	33%	3.6	11%
(1,2)	−19	4	16	−20.8	1.3	10	−22.3	3	16%	1.5	7%
(2,3)	−16.9	1.1	16	−17.1	0.8	11	−18.3	1.4	8%	1.2	7%
(3,4)	−13.1	2.6	9	−13.3	1.5	6	−13.0	0.1	8	0.3	2%
(4,5)	−11.2	2.0	8	−11.9	0.8	5	−12.0	0.8	7%	0.1	8
(5,6)	−11	4	4	−11.2	0.7	2	−10.2	1	9%	1	9%
(6,7)	−9.7	2.7	3	−10.3		1	−10.4	0.7	7%	0.1	1%

[a] The deviations are calculated after rounding the computed averages to the same significant figure as the correspondent data average (e.g., $\langle\Delta H^0_{0,1}\rangle$ is approximated to 40kcal/mol when calculating da_1 and to 37.0 kcal/mol when estimating da_1'). See text for explanation of symbols. For the present purpose, the calculated values are estimated at standard conditions (i.e., $T = 285.16$ K, $p = 1$ atm). $-\overline{\Delta H^0_{-1,0}} = -\overline{\Delta H^0_{-1,0}}' = (PA_{H_2O})_{meas}$ and $-\langle\Delta H^0_{n-1,n}\rangle = (PA_{H_2O})_{calc}$. [b] The indexes are with accordance to reaction 2 and refer to water protonation. [c] From Hunter and Lias.[22]

purpose, in Table 1 are reported the experimental data mean values, $\overline{\Delta H^0_{n-1,n}}$, and the corresponding standard deviations, σ_n, computed using all of the available experimental data,[23−45] $\Delta H^0_{n-1,n}$, for the reactions (2)

$$H_3O^+\cdot(H_2O)_{n-1} + H_2O \rightleftharpoons H_3O^+\cdot(H_2O)_n \qquad (2)$$

together with the number of data points, N, employed. The standard deviations, σ_n, have been assumed as the data sets averages, $\overline{\Delta H^0_{n-1,n}}$, uncertainties. Correspondingly, the data set averages have been rounded to the most significant figure consistent with their errors. In the same table are also reported the ensemble-averaged enthalpy estimates derived in this study, $\langle\Delta H^0_{n-1,n}\rangle$ (the word ensemble is here used to identify the set of non equivalent configurations that we were able to optimize for each specific cluster type), and their absolute and relative deviations from the corresponding experimental means, da_n and dr_n respectively. The absolute deviations are equal or smaller than σ_n for all n considered.

The largest deviation of our calculated values from the data averages, $\overline{\Delta H^0_{n-1,n}}$, is for addition of the first water ligand. This large deviation is partly due to the calculation technique and partly to the wide scattering of the data sets for (0,1), for which $\sigma_n = 10$ kcal/mol. To better assess the computational error, a restricted data set has been built which retains only those data which deviate from the average experimental values less than one standard deviation. The reduced data set has been used to calculate new enthalpy data averages, $\overline{\Delta H^0_{n-1,n}}'$, and new standard deviations, σ_n'. These are reported in Table 1 along with the absolute deviation of the computed values from the restricted data set, da_n', the percent deviation, dr_n' and the number of data points N' used to calculate data averages and standard deviations.

In Figure 2, the restricted data sets are plotted together with their averages and standard deviations (filled diamond symbols with error bars), with results from our simulations (filled circle symbols with error bars, labeled as QMsimA for quantum mechanical simulations averaged) and results from a macroscopic charged liquid drop model[46] (asterisks, labeled as Thomson model). When the restricted data set is considered, the deviations of the computed values from the data averages generally improve, in particular for $n = 1$ the deviation decreases from $da_1 = 10$ kcal/mol to $da_1' = 3.6$ kcal/mol. The latter value is still significantly larger than any of the others and thus still reflects the scattering in the different data sets. Hence, a smaller

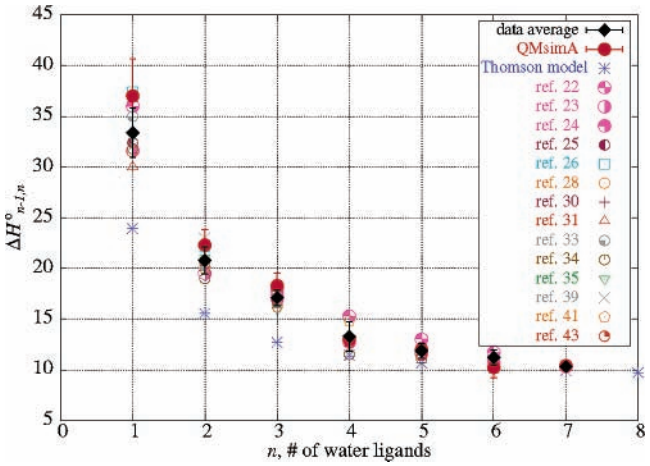

Figure 2. Restricted data sets plotted along with the data averages, $\overline{\Delta H^0_{n-1,n}}' \pm \sigma_n'$, the quantum mechanical simulations results averaged on the different isomers found, $\langle\Delta H^0_{n-1,n}\rangle \pm da_n$ (QMsimA), and the classical liquid charged droplet model due to Thomson.[46]

value will be assumed as representative of the computational error. An uncertainty of 3 kcal/mol has been chosen. Such values correspond to da_1' when dr_1' is set to 9%.

In Table 2, different determinations of the proton affinity of nitric acid from cited literature and computed in the present work are given. The left side of the table reports measured values, their references, and experimental method, whereas the right side reports computed values, their references, and the computational method employed. In particular, on the right side of the table is a value obtained by Lee and Rice[12] using CCSD(T)/DZP method and our results obtained using respectively: B3LYP/6-311++G(d,p), B3LYP/DZP, B3LYP/6-311+G(3df,2p), MP2/6-311++G(d,p), MP2/DZP, MP2/6-311+G(3df,2p), and G2 level of theories. The result of Lee and Rice[12] and the B3LYP/6-311++G(d,p), B3LYP/6-311+G(3df,2p), and G2 results bracket most experimental data, whereas MP2 values deviate substantially (although the use of the 6-311+G(3df,2p) larger basis set seem to reduce the disagreement).

Structures. The hydronium ion−water clusters and the mixed clusters will be discussed in turn.

Hydronium Ion−Water Clusters. The hydronium ion and its hydrated form, $H_5O_2^+$, have been the subject of many theoretical investigations (e.g., refs 19 and 47−51) and of a laboratory study.[17−19] Our results are in general agreement with

TABLE 2: Proton Affinity in kcal/mol of Nitric Acid from Experimental Determination and Computed

experimental data			computed data		
PA_{HNO_3}	ref.	method	PA_{HNO_3}	ref.	method
176 ± 7	11	FA[a]	182.5 ± 4	12	CCSD(T)/DZP
168 ± 3	14	ICR b.t.[b]	168.3	this work	B3LYP/DZP
177.7 ± 2.3	16	FA	175 ± 3	this work	B3LYP/6-311++G(d,p)
182.0 ± 2.3	15	FT-ICR[c]	175.1	this work	B3LYP/6-311+G(3df,2p)
			190.8	this work	MP2/DZP
			196.5	this work	MP2/6-311++G(d,p)
			189.3	this work	MP2/6-311+G(3df,2p)
			179.2	this work	G2

[a] Flowing afterglow. [b] Ion cyclotron resonance bracketing technique. [c] Fourier transform/chemical ionization mass spectrometry.

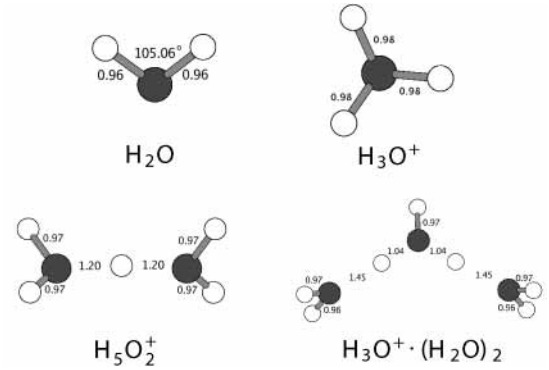

Figure 3. Graphical representation of protonated water and its two first hydrates. Distances are reported here and henceforth in Å.

the existing literature. The formation of a hydronium ion, C_{3v} H_3O^+, from H^+ and H_2O is a very exothermic process. The negative value of the enthalpy change associated with this process at standard conditions represents the proton affinity of water (see Table 1). Condensation of the hydronium ion to water forms $H_5O_2^+$. In this structure, of symmetry C_2, the proton is equally shared among the two water molecules. Some authors (e.g., refs 49 and 50) have succeeded in optimizing a structure of symmetry C_s for the hydrated hydronium ion in which the proton is more closely associated with one of the water molecules in a pyramidal configuration (similar to that of the hydronium ion). Such a configuration represents the minimum energy structure when optimizations are obtained with Hartree−Fock methods, whereas the C_2 structure is slightly higher in energy and corresponds to a transitional state. However, when theoretical methods that include electron correlation are used, the situation is reversed.[49] For this particular cluster, in the present study, MP2/6-311++G(d,p) structure optimizations were obtained. At both levels of theory, i.e., MP2/6-311++G(d,p) and B3YLP/6-311++G(d,p), the C_2 structure was the only one optimized. For more than two water ligands about the proton, the optimized structures are a series of H_3O^+ or $H_5O_2^+$ centered structures, the first being more predominant. For $H_7O_3^+$, the only structure found is hydronium coordinated to two waters. As a consequence of the water ligands, the oxygen−hydrogen bonds in the hydronium ion stretch from a typical distance of 0.98 Å in H_3O^+ to 1.04 Å. The structures are shown in Figure 3 together with the optimized structure for the water molecule.

For $H_9O_4^+$, three different structures were found. The isomers are shown in Figure 4 in order of decreasing stability. The D_{3h} hydronium centered structure is the lowest in energy (energies are electronic plus zero-point and thermal energy corrections for 156 K). $H_5O_2^+ \cdot (H_2O)_2$ is about 2 kcal/mol higher in energy. The ring-like structure, $H_3O^+ \cdot (H_2O)_{3_{II}}$, is organized about the hydronium ion to maximize the possible hydrogen bondings between the ligands. The contribution of the latter isomer to

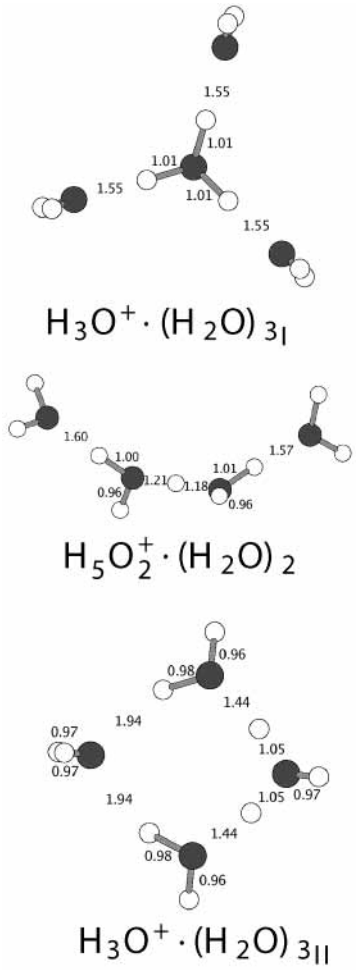

Figure 4. Three energy minima for the cluster $H^+ \cdot (H_2O)_4$. The relative energies to the $H_3O^+ \cdot (H_2O)_{3_I}$ structure are respectively: $E_{r,I} = 0$kcal/mol, $E_{r,H_5O_2^+ \cdot (H_2O)_2} = 2.0$ kcal/mol, and $E_{r,II} = 5.4$ kcal/mol.

the average cluster energy is negligible. When a Boltzmann average is performed, the three structures would be present in 99.8%, 1.8%, and less than 3×10^{-6}%, respectively.

The optimized $H_{11}O_5^+$ structures are shown in Figure 5. The most stable structure, $H_3O^+ \cdot (H_2O)_{4_I}$, is obtained by adding a water ligand to the first solvation shell of $H_3O^+ \cdot (H_2O)_{3_I}$ of Figure 4. A less stable isomer, $H_3O^+ \cdot (H_2O)_{4_{II}}$, is obtained from the starting geometry of $H_5O_2^+ \cdot (H_2O)_2$ to which a water ligand is added to one of the outer water ligands. In the resulting optimized geometry, the $H_5O_2^+$ core is distorted in such a way that the proton is no longer equally shared by two waters; instead, the proton preferentially migrates toward the one water with two water ligands added thus reforming a hydronium centered structure. The last structure, $H_3O^+ \cdot (H_2O)_{4_{III}}$, is a variation of the first and is about 3 kcal/mol higher in energy.

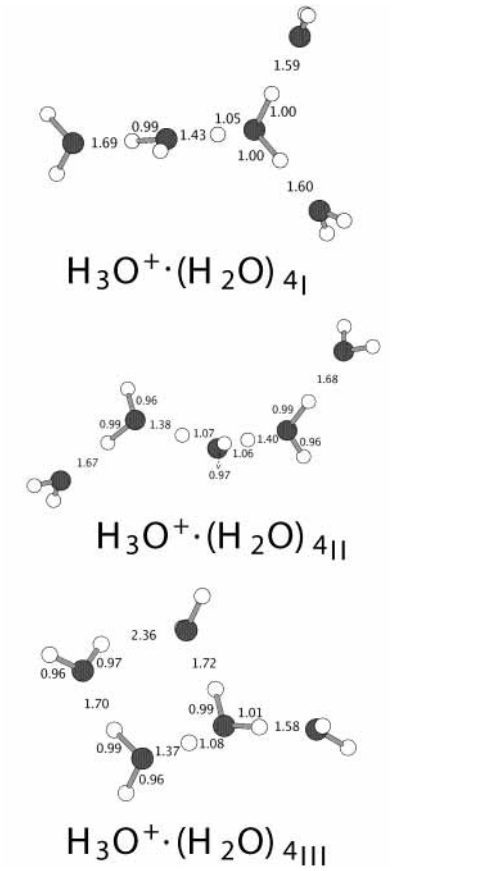

Figure 5. Optimized structures for four water ligand about the hydronium ion (or $H_{11}O_5^+$). The relative energies to the $H_3O^+\cdot(H_2O)_{4_I}$ structures are respectively: $E_{r,I} = 0$ kcal/mol, $E_{r,II} = 2.4$ kcal/mol, and $E_{r,III} = 2.9$ kcal/mol.

In this structure, the one water ligand beyond the first completed solvation shell is bonded in a ring-like fashion to two of the outer waters composing the shell.

The lowest structure in energy optimized for $H_{13}O^+_6$ is $H_5O_2^+$ centered. Three other structures were found which are variations on the first hydration shell structure with two waters added. The structures are shown in Figure 6. The energy difference between the first two lowest energy structures (the top two isomers shown in Figure 6) is of only about 0.6 kcal/mol. In a previous study of the hydronium ion−water clusters, Wei and Salahub[47] identified, for $H_{13}O^+_6$, two structures that correspond to the $H_5O_2^+\cdot(H_2O)_4$ and $H_3O^+\cdot(H_2O)_{5_I}$ isomers of Figure 6. In their calculations using the Perdew functional in the program "deMon"[52] with a DZVP basis set, the hydronium ion centered structure is lower in energy than the other structure by about 1kcal/mol.

For $H_{15}O_7^+$, the most stable structure optimized is a hydronium ion centered one and represents what has been indicated by Price[18] as the completed second solvation shell about the ion. In this structure, one additional water is added to each water in the first solvation shell of $H_3O^+\cdot(H_2O)_{3_I}$. The second stable structure optimized is only about 0.5 kcal/mol higher in energy than the lowest. The other two structures optimized are variations of the preceding isomers. They contribute negligibly to the cluster averaged properties.

For $H_{17}O_8^+$ four structures have been optimized and are shown in Figure 8. The total energy difference between the first two isomers is of about 0.6 kcal/mol. The other and less stable two structures are alternative ways of filling the second ion solvation shell.

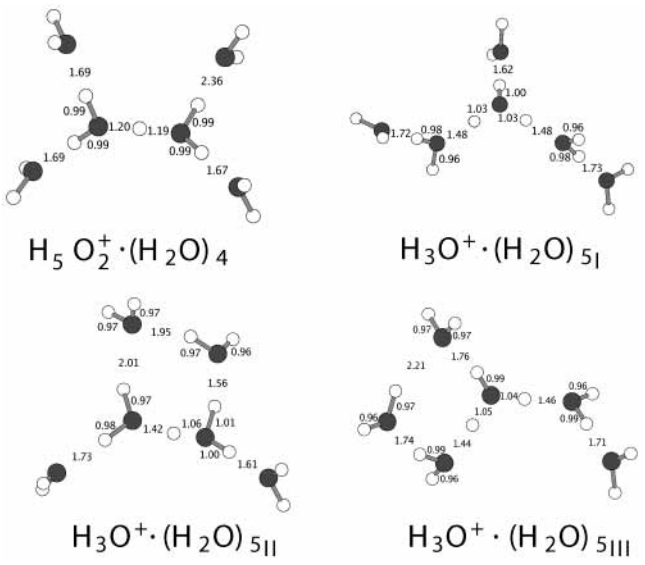

Figure 6. Optimized structures for five water ligands about the hydronium ion (or $H_{13}O^+_6$). The energies relative to the $H_5O_2^+\cdot(H_2O)_4$ structure are respectively: $E_{r,H_5O_2^+\cdot(H_2O)_4} = 0$ kcal/mol, $E_{r,I} = 0.6$ kcal/mol, $E_{r,II} = 1.4$ kcal/mol, and $E_{r,III} = 3.0$ kcal/mol.

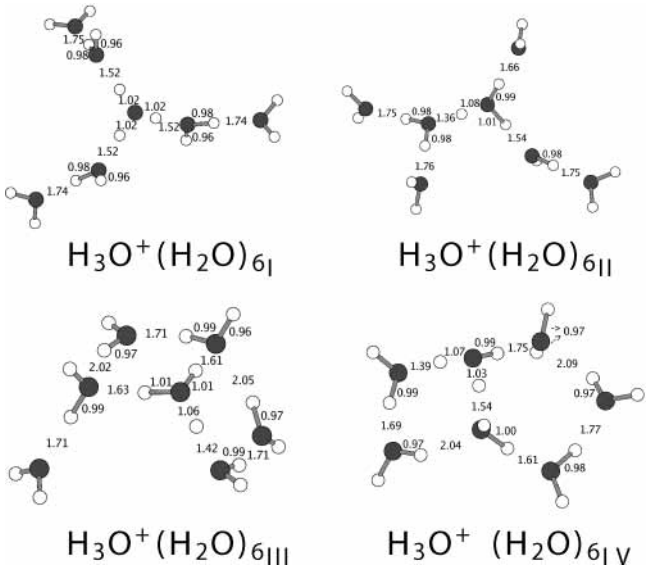

Figure 7. Optimized structures for six water ligands about the hydronium ion (or $H_{15}O_7^+$). The relative energies with respect to the $H_3O^+\cdot(H_2O)_{6_I}$ structure are, respectively: $E_{r,I} = 0$ kcal/mol, $E_{r,II} = 0.5$ kcal/mol, $E_{r,III} = 2.0$ kcal/mol, and $E_{r,IV} = 4.0$ kcal/mol.

For $H_{19}O_9^+$ four structures were optimized and are shown in Figure 9. The most stable isomer, $H_5O_2^+\cdot(H_2O)_7$, is obtained from $H_3O^+\cdot(H_2O)_{7_I}$ adding the extra water ligand in order to form a highly symmetrical structure centered on $H_5O_2^+$. The $H_3O^+\cdot(H_2O)_{7_I}$ isomer, very close in energy to the former, is H_3O^+ centered.

In general, protonated water cluster structures characterized by the presence of the $H_5O_2^+$ ion are very symmetrical structures; that is, they are characterized by the same number of waters coordinated to each of the four hydrogen ends of the ion. Whenever the symmetry is broken, the shared proton tends to migrate closer to the one water molecule in the ion to which more water ligands are hydrogen bonded. At the same time, the distance between the oxygen of the newly rearranged hydronium ion and its hydrogen, to which an excess of water molecules are bonded, lengthens. This is what happens going

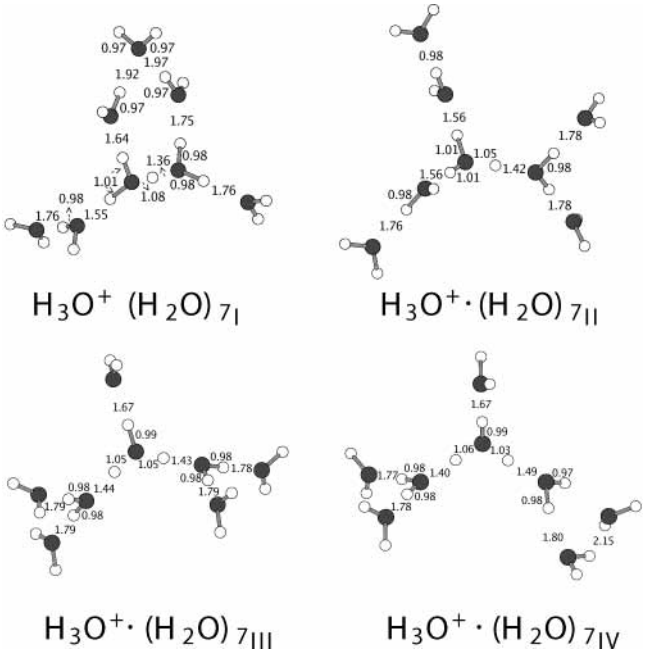

Figure 8. Optimized structures for 7 water ligands about the hydronium ion (or $H_{17}O_8^+$). The relative energies to the $H_3O^+ \cdot (H_2O)_{7_I}$ structure are respectively: $E_{r,I} = 0$ kcal/mol, $E_{r,II} = 0.6$ kcal/mol, $E_{r,III} = 1.7$ kcal/mol, and $E_{r,IV} = 3.2$ kcal/mol.

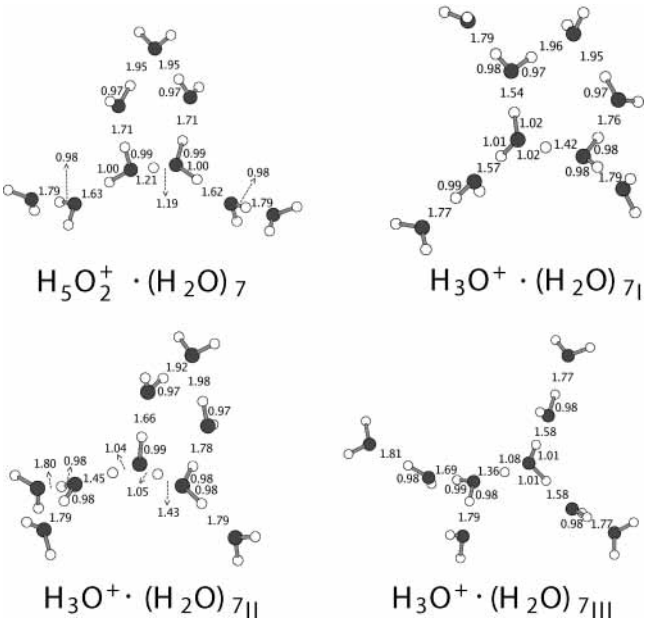

Figure 9. Optimized structures for 8 water ligands about the hydronium ion (or $H_{18}O_9^+$). The relative energies to the $H_3O^+ \cdot (H_2O)_{7_I}$ structure are respectively: $E_{r,H_5O_2^+ \cdot (H_2O)_7} = 0$ kcal/mol, $E_{r,I} = 0.7$ kcal/mol, $E_{r,II} = 1.1$ kcal/mol, and $E_{r,III} = 1.8$ kcal/mol.

from $H_5O_2^+$ to $H_3O^+ \cdot (H_2O)_3$, from $H_5O_2^+ \cdot (H_2O)_2$ to $H_3O^+ \cdot (H_2O)_{4_{II}}$, and from $H_5O_2^+ \cdot (H_2O)_4$ to $H_3O^+ \cdot (H_2O)_{6_{II}}$. This behavior is an exemplification of the hydrogen bond cooperativity. Whenever an excess water is added and a new hydrogen bond is formed within the aggregate, the water molecule to which the new ligand is added becomes a proton donor and, consequently, a better proton acceptor toward the water or hydronium ion to which it was already bonded. Accordingly, the O···O distance between the latter molecules shortens, whereas the O−H of the proton donor lengthens. This rearrangement propagates throughout the cluster. It is believed that such rearrangement is responsible for a stronger intermolecular

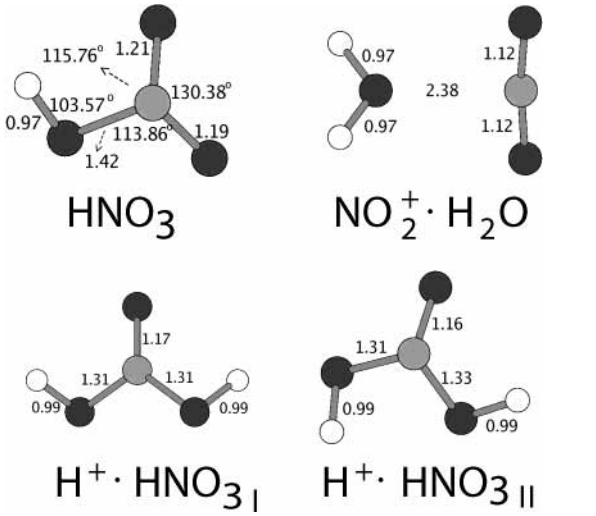

Figure 10. Optimized structures for nitric acid and protonated nitric acid. The first structure on the left is the most stable isomer. The relative energies to the $NO_2^+ \cdot H_2O$ structures are, respectively: $E_{r,NO_2^+ \cdot H_2O} =$ 0kcal/mol, $E_{r,I} = 18$ kcal/mol, and $E_{r,II} = 19$ kcal/mol.

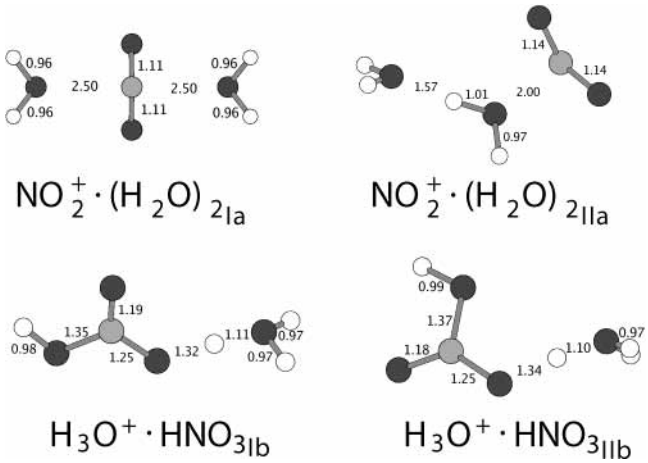

Figure 11. Optimized structures for hydrated protonated nitric acid. The first structure on the left is the most stable isomer. The energies relative to the $NO_2^+ \cdot (H_2O)_{2_{Ia}}$ structure are, respectively: $E_{r,Ia} = 0$ kcal/mol, $E_{r,IIa} = 0.3$ kcal/mol, $E_{r,Ib} = 1$ kcal/mol, and $E_{r,IIb} = 2$ kcal/mol.

cohesion resulting in a more stable aggregate with respect to the hypothetical cluster that had not undergone rearrangement.[56] The cooperativity of the hydrogen bonds within the computed protonated water clusters had been previously noted by other authors.[55,54] These observations are in some disagreement with the conclusions drown by Wei and Salahub:[47] "The length of O−H bonds within the hydronium ion decreases, whereas the hydrogen bond lengths between water and the hydronium unit increase as the cluster size increases. This is in good indication that the hydrogen bonds become weaker while the O−H bonds in the hydronium unit become stronger." In fact, the present results do show that the O···O distance between progressively peripheral water ligands increases with the cluster size but also show that (1) the O−H distance within the hydronium ion unit generally increases with the cluster size (see, for example, the symmetric structures about the hydronium ion core $H_3O^+ \cdot (H_2O)_{3_I}$, $H_3O^+ \cdot (H_2O)_{6_I}$) and (2) the O···O distance between the hydronium ion and its neighboring water molecules can either increase or decrease making the hydrogen bond weaker or stronger, respectively. In particular, the O···O distance between the O atom belonging to the hydronium ion and the oxygen of

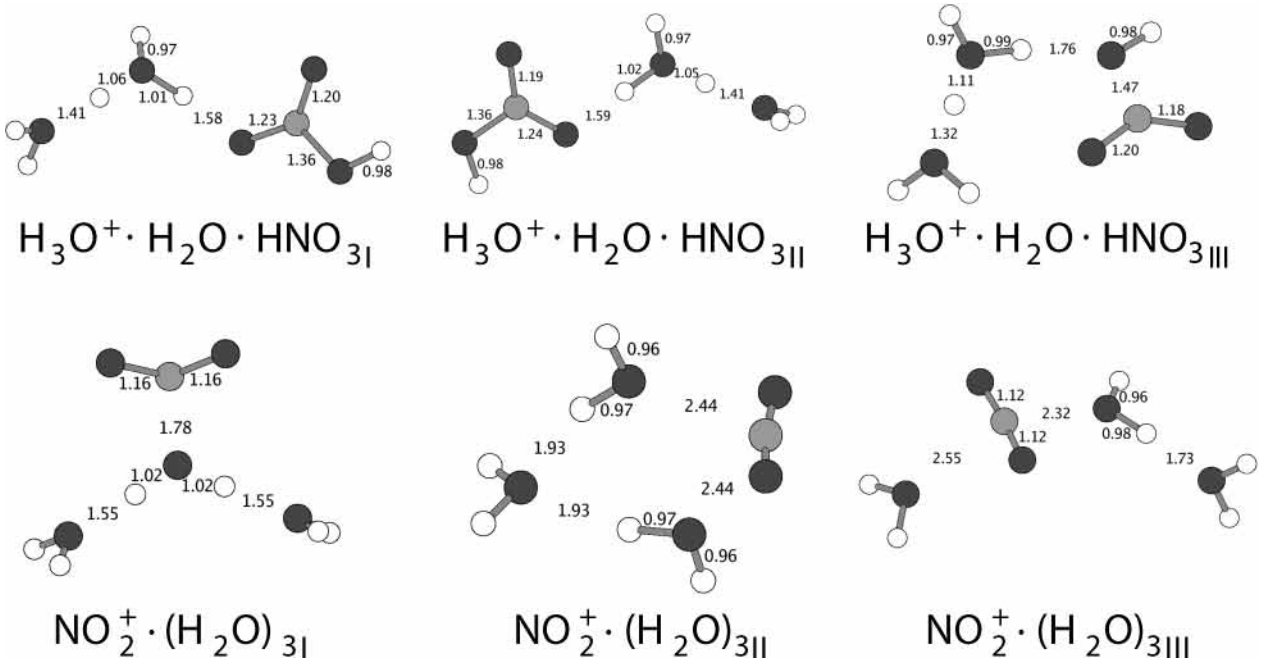

Figure 12. Optimized structures for dehydrated protonated nitric acid. The first structure on the upper left corner is the most stable isomer. The energies relative to the $H_3O^+\cdot H_2O\cdot HNO_{3_I}$ structure are, respectively: $E_{r,H_3O^+_I} = 0$ kcal/mol, $E_{r,H_3O^+_{II}} = 0.3$ kcal/mol, $E_{r,H^+\cdot HNO_3\cdot H_2O} = 3$ kcal/mol, $E_{r,NO(2/+)_I} = 5$ kcal/mol, $E_{r,NO(2/+)_{II}} = 9$ kcal/mol, and $E_{r,NO(2/+)_{II}} = 10$ kcal/mol.

one of the first neighboring waters shortens when such neighboring water (or a water H-bonded to it) forms a new hydrogen bond, thus becoming a proton donor with respect to the new H bond and hence a better proton acceptor with respect to the H-bond directed toward the hydronium ion. Shortening of the O···O distance implies a strengthening of the H bond. Conversely, the O···O distance lengthens when a new hydrogen bond forms that does involve other first neighboring waters to the hydronium ion than the one for which the O···O distance is considered. In the latter case, the hydrogen bond(s) with the other(s) water neighbor(s) is(are) strengthened at the expenses of the one under consideration.

Mixed Clusters. When protonated water clusters are exposed to a mixture of water and nitric acid vapors, the hydronium ion transfers a proton to nitric acid. This process is a consequence of the difference in the water and nitric acid proton affinities: the latter is about 10 kcal/mol higher than the former. As discussed previously, when the protonated nitric acid becomes hydrated, charge exchange reactions result in the formation of the hydronium ion−water cluster series at the expense of the mixed aggregate family. In the next two subsections, the structure characteristics and their properties are discussed in detail.

Charge Arrangements of the Mixed Clusters Depends on the Degree of Hydration. Both experiments[3−5,13,14] and ab initio calculations[12] show that protonated nitric acid exists in two isomeric forms. One of these is an ionic cluster of the nitronium ion and water, $NO_2^+\cdot H_2O$, whereas the other is nitric acid protonated at one O to give $(HO)_2NO^+$. The latter has two lower energy conformers. Geometry optimizations carried out in this study gave the three stable minima shown in Figure 10. The most stable isomer is the hydrated nitronium ion, $NO_2^+\cdot H_2O$, whereas the two conformational isomers of $(HO)_2NO^+$ are nearly 20 kcal/mol higher in energy. Cacace et al.[13] have reported that the isomerization of $(HO)_2NO^+$ structures into the $NO_2^+\cdot H_2O$ form is a slow process characterized by a high energy activation barrier. Thus, the $(HO)_2NO^+$ isomers may be important upon further hydration.

The isomers of protonated nitric acid solvated by one water molecule found in this study are shown in Figure 11. The most stable structures are dehydrated nitronium ions, $NO_2^+\cdot(H_2O)_{2_{Ia}}$ and $NO_2^+\cdot(H_2O)_{2_{IIa}}$ were found. The structures involving a hydronium ion hydrogen bonded to nitric acid are 1−2 kcal/mol less stable. Okumura and co-workers[3−5] studied the behavior of hydrated protonated nitric acid and observed that the preferred vibrational dissociation channel is by water evaporation, thus confirming the prediction that the NO_2^+ based structures are the most stable.

The structures of protonated nitric acid solvated by two water molecules are shown in Figure 12. The most stable isomer is now a hydronium ion solvated by a water and a nitric acid. The lowest energy solvated nitronium ion found is less stable than the hydronium centered ion by about 5 kcal/mol. This result does not agree with the experimental observation of Cao et al.,[3,4] who found that for dehydrated protonated nitric acid evaporation of water by vibrational excitation is the major dissociation channel. However, the authors did observe this kind of cluster dissociation of nitric acid upon vibrational excitation accounting for at least 15% of the photofragments. This indicates that about some 15% of the cluster isomers are characterized by the presence of the hydronium ion rather than the nitronium ion. Furthermore, the most stable isomeric configurations could dissociate to $H_5O_2^+ + HNO_3$ or $H_2O + H_2O\cdots H\cdots ONOOH$.

Upon further hydration, the hydronium ion plus nitric acid becomes more stable than the protonated nitric acid. For $H^+\cdot HNO_3\cdot(H_2O)_3$, the energy difference between the most stable hydronium ion based structure and the nitronium ion one is 16 kcal/mol. For $H^+\cdot HNO_3\cdot(H_2O)_4$, the energy difference increments to 18 kcal/mol. Thus, for these clusters, the hydronium ion based structures are most stable. This results agree with the experimental findings of Okumura and co-workers.[3,4]

As noted, the nitronium ion is the favored ion center for low level of hydration ($H^+HNO_3\cdot(H_2O)_n$, with $n = 0, 1$), whereas the hydronium ion is the preferred charge cation for a higher level of hydration. Cao et al.[4] have attributed this feature to the fact that water binds more strongly than nitric acid to the

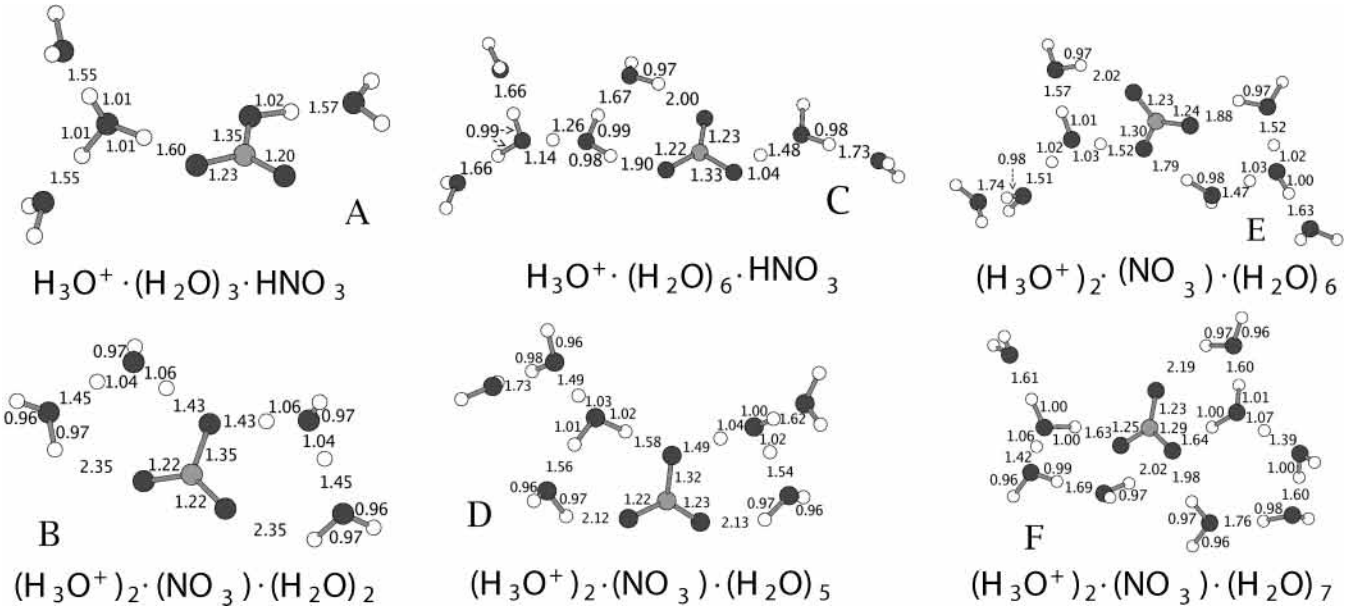

Figure 13. Structures of some protonated nitric acid−water clusters for 4−9 water molecules. The structures designated by the letters A, B, C, and D are different isomers of $H^+ \cdot (H_2O)_4 \cdot HNO_3$ and $H^+ \cdot (H_2O)_7 \cdot HNO_3$ respectively. E and F are the most stable structures for $H^+ \cdot (H_2O)_8 \cdot HNO_3$ and $H^+ \cdot (H_2O)_9 \cdot HNO_3$, respectively. The energies relative to their corresponding most stable isomers are respectively: $E_{r,A} = 0$ kcal/mol, $E_{r,B} = 6$ kcal/mol, $E_{r,C} = 0$ kcal/mol, $E_{r,D} = 0.5$ kcal/mol, $E_{r,E} = 0$ kcal/mol, and $E_{r,F} = 0$ kcal/mol.

hydronium ion. However, the authors apply this line of reasoning only to the $H^+ \cdot HNO_3 \cdot (H_2O)_n$ for $n \geq 3$ although water binds more strongly to the hydronium ion than nitric acid does even for $n = 1$. In conclusion, we have found that the charge center is in the form of the hydronium ion for $n \geq 2$ in $H^+ \cdot HNO_3 \cdot (H_2O)_n$, whereas Okumura and co-workers[3,4] have observed the same behavior but for $n \geq 3$. Wei et al.[53] have observed that the hydronium ion forms as the core ion "whenever the cluster is large enough to form a closed hydrogen-bonded shell structure". This happens in our study when $n = 3$ (in the formula $H_3O^+ \cdot (H_2O)_n \cdot HNO_3$).

Dissociation of Nitric Acid in Water Clusters. Figure 13 shows the most stable isomers and selected higher energy isomers of mixed clusters with different levels of hydration. Hydration causes onset of HNO_3 dissociation in the hydronium ion−water−nitric acid mixed cluster and eventual formation of a second hydronium ion plus a nitrate anion charge centers in large clusters. The dissolution of protonated nitric acid is affected by hydrogen bond cooperativity. The proton in the O−H group in the acid gets progressively stripped from its original oxygen as the number of water ligands increases. The O−H distance goes from 0.97 Å in HNO_3, see Figure 10, to 1.02 Å in structure A of Figure 13, to 1.04 Å of structure C, and to longer distances for larger clusters. The first cluster that we optimized in which two hydronium ions and one nitrate anion are present is a less stable isomer of $H_3O^+ \cdot (H_2O)_3 \cdot HNO_3$ (structure B of Figure 13). $(H_3O^+)_2 \cdot NO_3^- \cdot (H_2O)_5$ is less than 1 kcal/mol higher in energy than its more stable isomer $H_3O^+ \cdot (H_2O)_6 \cdot HNO_3$. For $H_3O^+ \cdot (H_2O)_n \cdot HNO_3$, with $n = 7$, 8, the $(H_3O^+)_2 \cdot NO_3^- \cdot (H_2O)_m$ structures, with $m = 6$, 7, are the most stable ones. Nitric acid tends to transfer a proton whenever it is surrounded by water ligands. Interestingly, the dissociation of nitric acid into the hydronium ion−water cluster begins at the number of water ligands nearly equal to the number for which we observe the onset of ligand exchange reactions in the direction of the mixed clusters. In conclusion, we have observed that dissociation of nitric acid in hydrated hydronium ion molecular clusters becomes possible when nitric acid is encaged by waters.

Acknowledgment. We are grateful to the National Science Foundation for financial support of this research under Grants ATM-00-70847 (R.P.T.) and CHE-0240023 (K.N.H.). R.D. was also supported by the NASA Earth System Fellowship ESS/00-0000-0080.

References and Notes

(1) Zhang, X.; Mereand, E. L.; Castleman, A. W., Jr. *J. Phys. Chem.* **1994**, *98*, 3554.
(2) Gilligan, J. J.; Castleman, A. W., Jr. *J. Phys. Chem. A* **2001**, *105*, 5601.
(3) Cao, Y.; Choi, J.-H.; Haas, B.-M.; Johnson, M. S.; Okumura, M. *J. Chem. Phys.* **1993**, *99*, 9307.
(4) Cao, Y.; Choi, J.-H.; Haas, B.-M.; Okumura, M. *J. Phys. Chem.* **1994**, *98*, 12176.
(5) Choi, J.-H.; Kuwata, K. T.; Cao, Y.-B.; Haas, B.-M.; Okumura, M. *J. Phys. Chem. A* **1997**, *101*, 6753.
(6) Ferguson, E. E.; Fehsenfeld, F. C.; Albitron, D. L. *Gas-phase ion chemistry*; Bowers, M. T., Ed.; Academic Press: London, 1979; Vol. 1, pp 45−83.
(7) Eichkorn, S.; Wilhelm, S.; Aufmhoff, H.; Wohlfrom, K. H.; Arnold, F.; *Geophys. Res. Lett.* **2002**, *29*, 43−I.
(8) Hanson, D. R.; Eisele, F. L. *J. Geophys. Res.* **2002**, *107*, 10−I.
(9) Arnold, F.; Viggiano, A. A.; Schlager, H. *Nature 297*, 371. Arnold, F.; Krankowsky, D.; Marien, K. H. *Nature 267*, 30.
(10) Arijs, E. *Ann. Geophys. 1*, 149.
(11) Fehsenfeld, F. C.; Howard, C. J.; Schmeltekopf, A. L. *J. Chem. Phys.* **1975**, *63*, 2835.
(12) Lee, T. J.; Rice, J. E. *J. Phys. Chem.* **1992**, *96*, 650.
(13) Cacace, F.; Attinà, M.; de Petris, G. *J. Am. Chem. Soc.* **1989**, *111*, 5481.
(14) Cacace, F.; Attinà, M.; de Petris, G.; Speranza, M. *J. Am. Chem. Soc.* **1990**, *112*, 1014.
(15) Cacace, F.; Attinà, M.; de Petris, G.; Speranza, M. *J. Am. Chem. Soc.* **1994**, it *116*, 6413.
(16) Sunderlin, L. S.; Squires, R. R. *Chem. Phys. Lett.* **1993**, *212*, 307.
(17) Yeh, L. I.; Okumura, M.; Myers, J. D.; Price, J. M.; Lee, Y. T. *J. Chem. Phys.* **1989**, *91*, 7319.
(18) Price, J. M. Ph.D. Thesis, Lawrence Berkeley Laboratory, University of California, Berkeley, California, 1990.
(19) Jiang, J.-C.; Wang, Y.-S.; Chang, H.-C.; Lin, S. H.; Lee, Y. T.; Niedner-Schatteburg, G.; Chang, H.-C. *J. Am. Chem. Soc.* **2000**, *122*, 1398.
(20) Frisch, M. J.; Trucks, G. W.; Schlegel, H. B.; Scuseria, G. E.; Robb, M. A.; Cheeseman, J. R.; Zakrzewski, V. G.; Montgomery, J. A., Jr.; Stratmann, R. E.; Burant, J. C.; Dapprich, S.; Millam, J. M.; Daniels, A. D.; Kudin, K. N.; Strain, M. C.; Farkas, O.; Tomasi, J.; Barone, V.; Cossi, M.; Cammi, R.; Mennucci, B.; Pomelli, C.; Adamo, C.; Clifford, S.;

Ochterski, J.; Petersson, G. A.; Ayala, P. Y.; Cui, Q.; Morokuma, K.; Malick, D. K.; Rabuck, A. D.; Raghavachari, K.; Foresman, J. B.; Cioslowski, J.; Ortiz, J. V.; Stefanov, B. B.; Liu, G.; Liashenko, A.; Piskorz, P.; Komaromi, I.; Gomperts, R.; Martin, R. L.; Fox, D. J.; Keith, T.; Al-Laham, M. A.; Peng, C. Y.; Nanayakkara, A.; Gonzalez, C.; Challacombe, M.; Gill, P. M. W.; Johnson, B. G.; Chen, W.; Wong, M. W.; Andres, J. L.; Head-Gordon, M.; Replogle, E. S.; Pople, J. A. *Gaussian 98*; Gaussian, Inc.: Pittsburgh, PA, 1998.

(21) In a study regarding hydrogen peroxide compleses, Daza and coworkers have shown that the BSSE correction for their system when studied with DFT technique (B3LYP/6-311+G(3df, 2p)) ranged between 1.26 and 0.27 kcal/mol. Daza, M. C.; Dobado, J. A.; Molina Molina, J.; Salvador, P.; Duran, M.; Villaveces, J. L. *J. Chem. Phys.* **1999**, *110*, 11806. Note that our calculation of the nitric acid proton affinity with the same level of theory used by the aforementioned authors led to a result whose difference from the one obtained with B3LYP/6-311++G(d, p) calculations lies well within the computational error defined in our work (see Table 2).

(22) Hunter, E. P. L.; Lias, S. G. *J. Phys. Chem. Ref. Data* **1998**, *27*, 413.

(23) Kebarle, P.; Searles, S. K.; Zolla, A.; Scarborough, J.; Arshadi, M. *J. Am. Chem. Soc.* **1967**, *89*, 6393.

(24) Cunningham, A. J.; Payzant, J. D.; Kebarle, P. *J. Am. Chem. Soc.* **1972**, *94*, 7627.

(25) Lau, Y. K.; Ikuta, S.; Kebarle, P. *J. Am. Chem. Soc.* **1982**, *104*, 1462.

(26) Dalleska, N. F.; Honma, K.; Armentrout, P. B. *J. Am. Chem. Soc.* **1993**, *115*, 12125.

(27) Honma, K.; Sunderlin, L. S.; Armentrout, P. B. *J. Chem. Phys.* **1993**, *99*, 1623.

(28) Honma, K.; Sunderlin, L. S.; Armentrout, P. B. *Int. J. Mass Spectrom. Ion Proc.* **1992**, *117*, 237.

(29) Szulejko, J.; McMahon, T. B. personal communication, 1992.

(30) Magnera, T. F.; David, D. E.; Michl, J. *Chem. Phys. Lett.* **1991**, *182*, 363.

(31) Hop, C. E. C. A.; McMahon, T. B.; Willett, G. D. *Int. J. Mass Spectrom. Ion Proc.* **1990**, *101*, 191.

(32) Magnera, T. F.; David, D. E.; Stulik, D.; Orth, R. G.; Jorikman, H. T.; Michl, J. *J. Am. Chem. Soc.* **1989**, *111*, 5036.

(33) Shiromaru, H.; Shinohara, H.; Washida, N.; Yoo, H. S.; Kimura, N. *Chem. Phys. Lett.* **1987**, *141*, 7.

(34) Hiraoka, K.; Takimoto, H.; Morise, K. *J. Am. Chem. Soc.* **1986**, *108*, 5683.

(35) Meot-Ner, M.; Speller, C. V. *J. Phys. Chem.* **1986**, *90*, 6616.

(36) Meot-Ner, M.; Field, F. H. *J. Am. Chem. Soc.* **1977**, *99*, 998.

(37) Bennett, S. L.; Field, F. H. *J. Am. Chem. Soc.* **1972**, *94*, 5186.

(38) Beggs, D. P.; Field, F. H. *J. Am. Chem. Soc.* **1971**, *93*, 1567.

(39) Beggs, D. P.; Field, F. H. *J. Am. Chem. Soc.* **1971**, *93*, 1576.

(40) DePaz, M.; Leventhal, J. J.; Friedman, L. *J. Chem. Phys.* **1969**, *51*, 3748.

(41) Gheno, F.; Fitaire, M. *J. Chem. Phys.* **1987**, *87*, 953.

(42) Field, F. H. *J. Am. Chem. Soc.* **1969**, *91*, 2827.

(43) Tholman, D.; Tonner, D. S.; McMahon, T. B. *J. Phys. Chem.* **1994**, *98*, 2002.

(44) Arifov, U. A.; Pozharov, S. L.; Chernov, I. G.; Mukhamediev, Z. A. *High Energy Chem.* **1973**, *7*, 347.

(45) Shi, Z.; Ford, V.; Wei, S.; Castleman, A. W., Jr. *J. Chem. Phys.* **1993**, *99*, 8009.

(46) Thomson, J. J.; Thomson, G. P. *Conduction of electricity through gases*; Cambridge University Press: New York, 1928.

(47) Wei, D.; Salahub, D. R. *J. Chem. Phys.* **1994**, *101*, 7633.

(48) Wei, D.; Salahub, D. R. *J. Chem. Phys.* **1997**, *106*, 6086.

(49) Xie, Y.; Remington, R. B.; Schaefer, H. F., III. *J. Chem. Phys.* **1994**, *101*, 4878.

(50) Ojamäe, L.; Shavitt, I.; Singer, S. J. *Int. J. Quantum Chem., Quantum Chem. Symp.* **1995**, *29*, 657.

(51) Ojamäe, L.; Shavitt, I.; Singer, S. J. *J. Chem. Phys.* **1998**, *109*, 5547.

(52) St-Amant, A.; Salahub, D. R. *Chem. Phys. Lett.* **169**, *1990*, 378.

(53) Wei, S.; Tzeng, W. B.; Keese, R. G.; Castleman, A. W., Jr. *J. Am. Chem. Soc.* **1991**, *113*, 1960.

(54) Deakyne, C. A.; Meot-Ner, M.; Campbell, C. L.; Hughes, M. G.; Murphy, S. P. *J. Chem. Phys.* **1986**, *84*, 4958.

(55) Newton, M. D. *J. Chem. Phys.* **1977**, *67*, 5535.

(56) Frank, H. S. *Proc. R. Soc. London. Ser. A* **1957**, *247*, 481.